MECHANICAL AND THERMAL CHARACTERISTICS OF THE PARTICLES REINFORCED PHENOLIC FOAMS

S.A. Song, S.S. Kim*

ᵃDepartment of Organic Materials and Fiber Engineering, Chonbuk National University, Jeonju, 560-756, Republic of Korea.
* Corresponding author (sskim@jbnu.ac.kr)

Abstract
The commercial polymer foams such as polyurethane and polystyrene have low flame resistance and it generated the toxic gases. Recently, to solve this problem, phenolic resin is spotlighted due to excellent flame resistance, high thermal stability over a broad temperature range and low generation of toxic gases during combustion. However, the phenolic foam has inferior mechanical strength and high thermal conductivity compared with other polymer foams and it is difficult to control the cell morphology. In this work, the phenolic foam was fabricated by using microwave and nano-particles such as multiwall carbon nanotube (MWNT) and graphene were mixed to improve the thermal and mechanical properties of the phenolic foam. And to obtain the optimal cell morphology, proper foaming points of each particle reinforced phenolic foams were investigated by cure monitoring.

1. Introduction

Phenolic foams have high strength, excellent flame resistance, and low generation of toxic gases during combustion. They also have high self-ignition temperature of 480°C and high thermal stability over a broad temperature range, maintaing performance and stability from -196°C to 200°C. So it has led to a broad range of applications as an insulating material [1, 2]. However, the phenolic foams applications are limited by their inferior mechanical strength and high thermal conductivity compared with other polymer foams. They have rarely been used as a sandwich structures because the phenolic resin make it more difficult to control the cell morphology [3, 4, 5].
The physical performances of polymer foams were determined by their densities, cell sizes, and cell shapes [6, 7, 8, 9]. Many studies about polymer foams have focused on the improvement of physical properties. Song et al. studied the effect of viscosity on aluminum structure, pore distribution and pore diameter [10]. Several studies about particles reinforced polymer foams explained the effect of cell morphology change on the mechanical properties. However, the analysis about the effect of particle to cell formation is rare. Cell formation during the foaming process of the resin is influenced by cross link of polymers and viscosity because they can control the expansion of the resin in foaming process [10]. Accordingly, the cell morphology and cell uniformity are influenced by viscosity [10]. When the foam has large specific surface area, the foam has excellent performance as thermal insulation foam. And it has great thermal stability by low thermal conductivity. Total thermal conductivity in polymer foam is the sum of the conductivities of both the gas and solid [11, 12]. Radiative heat transfer happens through

cell walls so many small cells will transfer. The cell morphology has a larger impact to determine the mechanical and thermal poperties than just changing the density.

In this work, the phenolic foam was fabricated by using microwave and nano-particles such as multiwall carbon nanotube (MWNT) and graphene were mixed to improve the thermal and mechanical properties of the phenolic foam. And to obtain the optimal cell morphology, proper foaming points of each particle reinforced phenolic foams were investigated by cure monitoring.

2. Materials and experimental

2.1. Materials

Resole-type phenolic resins (OG-5000, Kangnam Chemical Co., Korea) were mixed with acid catalyst (PTSA 65%, Kangnam Chemical Co., Korea) and mixing ratio by weight is 9:1. And the mixture was stirred at 500rpm for 1minute using the impeller. Multi-wall carbon nanotube (724769, Sigma-Aldrich Co. LLC., USA) and graphene (C500, Hanwhananotech, Korea) were added to the phenolic resin at different weight fraction of 0.5, 1.0, and 2.0wt% respectively. Table 1 shows the physical properties of the phenolic resin and the reinforcing particles.

2.2. Cure monitoring

In our previous work, the foaming point of the phenolic resin using microwave was determined by cure monitoring to obtain the optimum cell morphology. From the result, the phenolic foam fabricated by applying the microwave at the cure starting point showed highly improved thermal and mechanical characteristics of the phenolic foams [12].

Based on the previous results, cure monitoring of the carbon nanoparticles reinforced phenolic resin was performed to decide the cure starting point with respect to the particle type and weight percent (wt%) at room temperature (20℃).MWCNT and graphene were applied to the phenolic resin at different weight percent of 0.5, 1.0, and 2.0 wt%, respectively, and their effect on the cure reaction of the phenolic resin was monitored. Each sample was named with respect to the particle type and weight percent as shown in Table 1. To estimate the degree of cure of the phenolic resins in accordance with the aging time after mixing the phenolic resins and accelerators using an impeller, a dielectric sensor (Lacomtech, Republic of Korea) and a K-type thermocouple (TT-K-30, OMEGA, USA) were used to measure the dissipation factor and the temperature, respectively. The dissipation factor D was measured in the phenolic resins using a commercial dielectrometer (ELC-133A, Escort Instruments Corp., USA) using a 1 kHz alternating current. At least three specimens were tested for each sample to obtain the repeatability of the results.

CP 0.5	0.5 wt% MWNT	CP 0.5	0.5 wt% Graphene
CP 1.0	1.0 wt% MWNT	CP 1.0	1.0 wt% Graphene
CP 2.0	2.0 wt% MWNT	CP 2.0	2.0 wt% Graphene

Table 1. Sample naming of the particles reinforced phenolic resins.

The isothermal differential scanning calorimetry (DSC), (Q20, TA Instruments, USA) experiments were carried out at room temperature to compare with cure monitoring results by using the dielectric sensor. All the samples were ramped from 15℃ to 25℃ with a heating rate of 5℃/min followed by holding at 25℃ for 50 min. This procedure is similar to the dielectric cure monitoring condition of the phenolic resin.
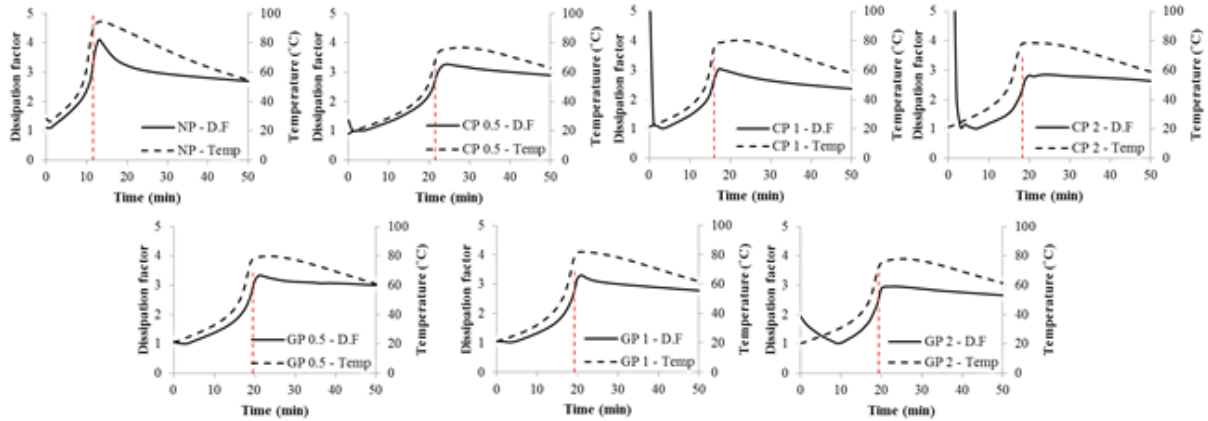
Figure 1. Dissipation factor and temperature profiles of the neat phenolic resin and the particle reinforced phenolic resins at room temperature

2.3. Foaming process

The microwave foaming was performed using the following three steps: (1) mixing the resole and accelerators with or without the particles using an impeller at 500 rpm for 3 min; (2) aging the mixture under constant room temperature to control the initial degree of cure before microwave foaming; and (3) foaming by microwave using an effective intensity per unit mass of 12 kW/kg at 2.4 GHz and de-molding [11, 12]. Aging time before microwave foaming was determined by the cure monitoring results of each sample.

2.4 Characterization

2.4.1 Foam density

The foam diameter and length to measure the foam density are 75 mm and 130 mm, respectively. The specimens are dried at 80°C for 2 h to remove the internal moisture before measuring the mass. In practice, the density (kg/m^3) of plastic foams is calculated as the ratio of specimen mass m to geometrical volume V as shown in the following equation:

$$\rho = \frac{M}{V} = \frac{kg}{\pi r^2 h} = \frac{kg}{m^3} \qquad (1)$$

Density of the solid specimen fabricated using phenolic resin was also measured to calculate the porosity of the phenolic foams.

2.4.2 Porosity

Porosity of the phenolic foams with respect to the test variables was calculated using the following equation (2). Where ρ_s and ρ_f are the previously measured solid density and foam density, respectively.

$$P = \frac{\rho_s - \rho_f}{\rho_s} \times 100\% \qquad (2)$$

2.4.3 Compressive test

A uniaxial compression test was conducted to measure the compressive strength. The cylindrical-shaped specimens of 16 mm in radius and 130 mm in length were fabricated using cylindrical acrylic mold. The compressive strength of the each sample with respect to the test variables was measured according to ASTM C 365 using a computer-controlled material testing system (4206, INSTRON, USA). To remove the water content, the specimens were dried at 80°C for 2 h before the test. The crosshead speed of the test was 0.5 mm/min.

2.4.4 Thermal conductivity

The thermal conductivity was measured using a hot-wire method based on the DIN 51046. To measure the thermal conductivity using the hot wire parallel technique, a constant electric current was applied throughout the nichrome wire (0.6 mm in diameter). The cylindrical-shaped specimen of 75 mm in diameter and 130 mm in length was initially placed.
A constant electric current with a 0.9 V (Voltage) was continuously applied to the specimens, and the temperature was measured using the thermocouple at time intervals ranging from 80 to 180 s. Using these data, the basic thermal conductivity was calculated with following equation [11, 12]:

$$k = \frac{q'}{4\pi} \times \frac{\ln\left(\frac{t_2}{t_1}\right)}{T_2 - T_1} \tag{3}$$

3. Result and discussion

Fig. 1 illustrates the dissipation factor and temperature of the phenolic resin during the cure reaction at room temperature with respect to the particle type and weight percent, and each graph shows the results of the representative specimen whose cure starting point is the closest to the average value of the three specimen in each test variable shown in Table 2. The cure starting point presented in each graph was determined as the inflection point at which the second derivative of the dissipation factor was zero ($d^2D/dt^2=0$) [13, 14].

Sample	Cure starting point (min)	Sample	Cure starting point (min)
NP	17.74		
CP 0.5	16.33	GP 0.5	17.59
CP 1.0	15.58	GP 1.0	17.37
CP 2.0	15.91	GP 2.0	17.51

Table 2. Cure starting point of neat phenolic resin and the particles reinforced phenolic resin.

Phenolic resin reinforced with the carbon nanoparticles showed low dissipation factor compared to that of the neat phenolic resin because the dipole and ion mobilities were restricted due to relatively high viscosity of the particle reinforced phenolic resin [13, 14]. Also the temperature at the cure starting point and the peak temperature of the particles reinforced phenolic resins were lower than those of the neat phenolic resin. This means the cure reaction of the particles reinforced phenolic resins progressed under lower temperature compared to the neat phenolic resin. And the cure reaction of particle reinforced phenolic resins is completed in short time as shown in Fig.2.
The neat phenolic resin showed the latest cure starting point. Graphene reinforced phenolic resin showed similar cure starting point regardless of the particle weight fraction as shown in Table 2, but MWNT reinforced phenolic resin showed a little different cure starting point with respect to the particle weight fraction. MWNT is more catalyze the cure reaction comparison with graphene. GP 0.5 showed the similar cure starting point with neat phenolic resin, while the CP 1.0 showed the fastest cure starting point. In case of the MWNT reinforced phenolic

resins, viscosity is relatively higher than the other graphene reinforced phenolic resins due to difference of aggregated shape of particle compared with graphene so that the cure catalyst effect of the MWNT on the cure reaction was more remarkable than the graphene reinforced phenolic resin. CP 1.0 sample have fast cure reaction comparison with CP 2.0, this means that the effect of the increasing viscosity by high particle contents on the dipole and ion mobilities comes to be dominant.
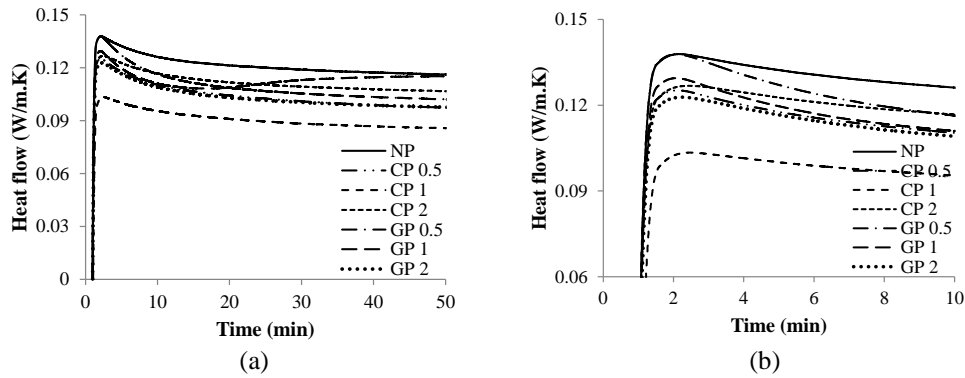

(a)   (b)

Figure 2. Isothermal DSC curve of the neat phenolic and particle reinforced phenolic resins: (a) isothermal scanning at 20˚C for 50min, (b) initial curing from 0 to 10 min.

DSC results were checked to confirm the cure behaviors of the particle reinforced phenolic foams derived from the dissipation factor. Fig. 2 shows the curing of the neat phenolic and the particles reinforced phenolic resins. The thermograms demonstrated typical isothermal behaviors in the cure reaction of thermoset polymers. It was found that the particles reinforced phenolic resins are faster in reaching the exothermic peak than the neat phenolic resin. To take a better look at the initial curing, the thermograms during the first 10 min are presented in Fig. 2(b). The time at the maximum heat flow peak shows the consistent with the result from dissipation factor and temperature measurement results. The two kinds of particles investigated here showed a difference in the initial curing stage as evidenced by the initial curing slopes and exothermic peak position.

Sample	Max peak (min)	Sample	Max peak (min)
NP	2.14		
CP 0.5	1.84	GP 0.5	1.93
CP 1.0	1.82	GP 1.0	1.76
CP 2.0	1.99	GP 2.0	1.83

Table 3. The time at the maximum exothermic peak (min) for isothermal scanning at room temperature (25˚C).

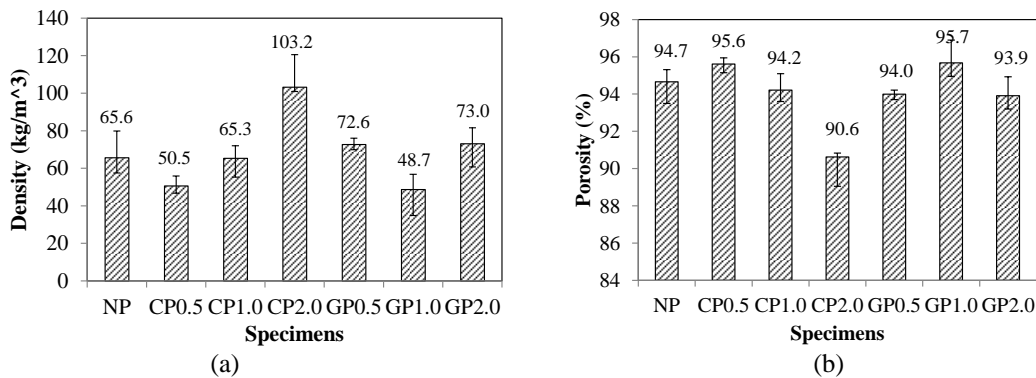(a)   (b)

Figure 3. Cell properties of the neat phenolic foam and particle reinforced phenolic foams: (a) density of the foams and solid, (b) porosity of the foams.

5

Table 3 shows the time at the maximum heat flow (min) for isothermal scanning at room temperature (25˚C). The heat flow data confirmed that the addition of the particles in the phenolic resin accelerated the cure to a certain degree.

Fig. 3 shows the density and porosity of the phenolic foams fabricated by microwave at the cure starting point shown in Table 2. Densities of the neat phenolic foam and the particles reinforced phenolic foams were various between 48.7 to 103.2 kg/m^3 as shown in Fig. 3(a). In case of the MWNT reinforced phenolic foams were increased the density with respect to increasing the weight fraction of particle. Because MWNT reinforced phenolic resins have extremely high viscosity with increasing the weight fraction of particle.

In case of the solid phenolic, density was decreased by addition of particles due to the internal void generation induced by the particle aggregation. Porosity of the phenolic foams calculated from measured solid and foam densities shows similar tendency with the foam density. CP 0.5 shows the highest porosity in the MWNT reinforced phenolic foams, but it is slightly lower than GP 1.0. And CP 2.0 shows the high foam density and low porosity due to extremely high viscosity.
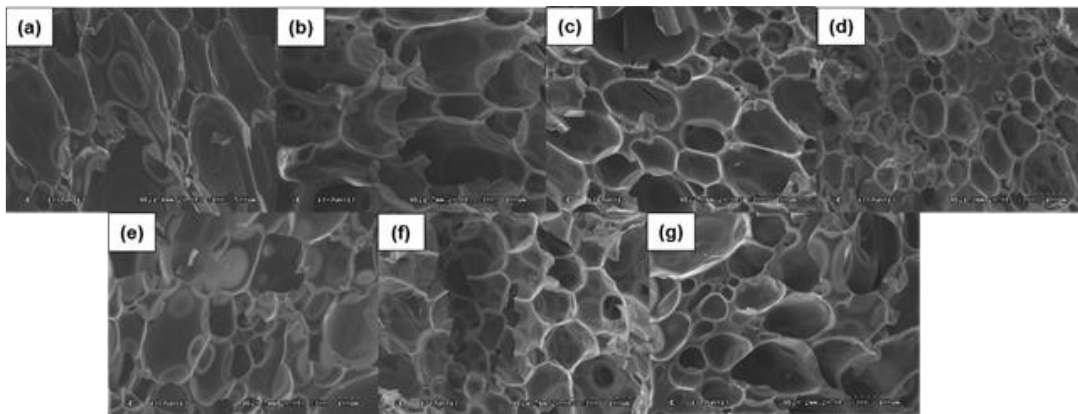

Figure 4. SEM topographies of the phenolic foams with respect to the particle type and weight fraction; (a) neat phenolic foam, (b)~(d) MWNT reinforced phenolic foam, (e)~(g) graphene reinforced phenolic foam.

Fig. 4 shows SEM images of the phenolic foams with respect to the particle type and weight fraction. Generally, polymer foams without any pressure during the foaming process show the anisotropic cell structures because the resin with foaming gases move to the top surface along the molding wall as the foaming process proceeds. The particles reinforced phenolic foams, however, show the entirely round cell structures and smaller cell size compared to the neat phenolic foam as shown in Fig. 4 (b)-(g). GP 1.0 shows thinner cell wall and small and uniform cell structures compared to the other particles reinforced foams. Thin cell walls are observed in the CP 0.5 and GP 0.5 although their cell sizes are relatively large. CP 2.0 and GP 2.0 have outstanding thick cell wall thickness due to high viscosity. And partially cell morphologies show very large cavities as shown in Fig. 4. Particles in the phenolic resin filled with high weight fraction of particles can be easily aggregated each other and the air at the tiny gaps between the aggregated particles expands dramatically as the microwave heating proceeds. This large bobbles are merged each other and then they make large cavities.

Fig. 6 shows the compressive strength and specific compress strength of the phenolic foams with respect to the particle type and weight fraction. All samples of particle reinforced phenolic foam were increased the specific compressive strength. In case of CP 2.0, it shows the highest compressive strength due to many solid parts. CP 0.5 and GP 1.0 which have high porosity and uniform cell morphology showed the highest specific compressive strength. Also cell density are closely related each other. Specific compressive strength of the CP 0.5 and GP 1.0 increased by 2.4 and 2.6 times, respectively, compared to the neat phenolic foam.
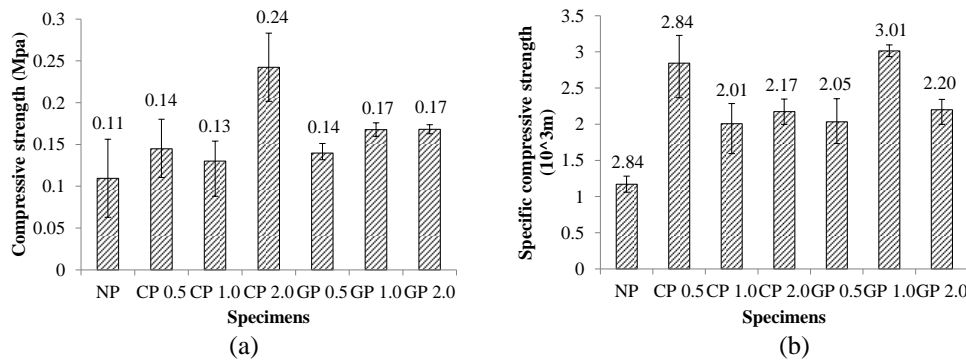
Figure 6. Compressive strength and specific compressive strength of the phenolic foams: (a) compressive strength, (b) specific compressive strength.

However the deviation of the specific compressive strength of the particles reinforced phenolic foams was much larger than that of the neat phenolic foam because of the partially large void induced by particle aggregation and stress shielding by thick cell wall [12]. The specific compressive strengths of the graphene reinforced phenolic foams were slightly higher than those of the MWNT reinforced phenolic foams, and this might be caused by a difference of aggregated shape of the particles.
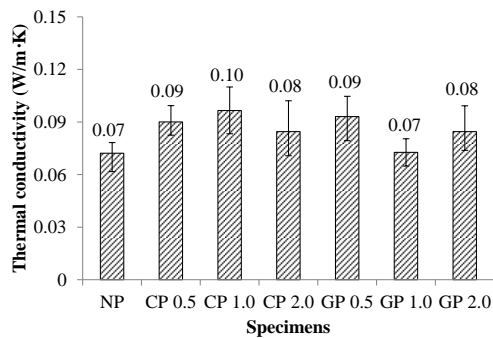

Figure 7. Thermal conductivities of neat phenolic foam and particle reinforced phenolic foams.

MWNT and graphene reinforced phenolic foams showed higher thermal conductivity compared to the neat phenolic foams due to the particles have remarkable high thermal conductivities. However, the thermal conductivity is slightly increased about 1.1 to 1.4 times compared to neat phenolic foam. That is insignificant comparison with increased specific compressive strength. Although the conductivity through gases is usually the predominant component of the total transferred heat due to the huge volume of the gaseous phase in foams, the main quantity of heat transferred of foams is the factor by conduction through the solid polymer [15, 16]. This means the thermal conductivity is affected by various factor as shown in Fig 7. Accordingly, phenolic foams with the lowest density (GP 1.0) showed the low thermal conductivities compared to the other foams and it is same to neat phenolic foam. In case of the GP1, which has the highest cell density and cell uniformity. However, CP2 and GP2, which has relatively low thermal conductivity duo to small cell size despite the partially thick cell walls due to the high viscosity before microwave foaming. And CP 0.5 has high thermal conductivity due to big cell size. Optimal cell morphology is important to decrease the thermal conductivity and it can be controlled by type of particle and weigh fraction of particle.

4. Conclusions

In this work, the particles reinforced phenolic foams were fabricated using microwave to improve the thermal and mechanical performance. From the experiments, the following results were obtained:

(1) Phenolic resin reinforced with the particles showed low dissipation factor compared to the neat phenolic resin because the dipole and ion mobilities were restricted due to relatively high viscosity of the particles reinforced phenolic resin.

(2) Density and porosity of the particles reinforced phenolic foams were lower than that of the neat phenolic foam due to the high cell density.

(3) CP 0.5 and GP 1.0 show thinner cell wall and small and uniform cell structures compared to the other particles reinforced foams.

(4) Specific compressive strength of the CP 0.5 and GP 1.0 increased by 2.4 and 2.6 times, respectively, compared to the neat phenolic foam.

(5) GP 1.0, which has the highest cell density and cell uniformity, has the lowest thermal conductivity in the phenolic foams and it is same to neat phenolic foam.

Our findings suggest that the graphene reinforced phenolic foams with 1wt%, fabricated using the proper foaming conditions, are promising materials for insulating foams due to their low thermal conductivity, low density, and reliable compressive strength.

References

[1] DK. Kim, SB. Lee "Properties and thermal characteristics of phenol foams for heat insulating materials". Journal of Korean Ind Eng Chem, Vol.17, pp 357-360, 2006.

[2] A. Desai, SR. Tutt "Modeling of fiber reinforced phenolic foam". Journal of cellular plastics, Vol. 44, pp 391-413, 2008.

[3] LJ. Gibson, MF. Ashby "Cellular solids: structure and properties". Oxford: Pergamon Press, Vol. 53, 1988.

[4] GD. Carvalho, JA. Pimenta, WN. Dos santos, E. Frollini "Phenolic and lignophnolic closed cells foams: Thernal conductivity and other properties". Polymer-plastics technology and engineering, Vol. 42, pp 605-626, 2003

[5] KA. Arora, AJ. Lesser, TJ. McCarthy "Preparation and characterization of microcellular polystyrene foams processed in supercritical carbon dioxide". Macromolecules, Vol. 31, pp 4614-4620, 1998.

[6] I. Javni, W. Zhang, V. Karajkov, ZS. Petrovic "Effect of nano- and micro-silica fillers on polyurethane foam properties". Journal of cellular plastics, Vol. 38, pp 229-239, 2002.

[7] CM. Stafford, TP. Russell, TJ. McCarthy "Expansion of polystyrene using supercritical carbon dioxide: effects of molecular weight, polydispersity, and low molecular weight components". Macromolecules, Vol. 32, pp 7610-7616, 1999.

[8] A. Desai, ML. Auad, H. Shen, SR. Nutt "Mechanical behavior of hybrid composite phenolic foam". Journal of cellular plastics, Vol. 44, pp 15-36, 2008.

[9] I. Javni, W. Zhang, V. Karajkov, ZS. Petrovic "Effect of nano-and micro-silica fillers on polyurethane foam properties". Journal of cellular plastics, Vol. 38, pp 229-239, 2002.

[10] ZL. Song, LQ. Ma, ZJ. Wu, DP. He "Effects of viscosity on cellular structure of foamed aluminum in foaming process", Journal of materials science, Vol. 35 pp 15-20, 2000.

[11] BC. Kim, SW. Park, DG. Lee "Fracture toughness of the nano-particle reinforced epoxy composite". Conposite structures, Vol. 86, pp 69-77, 2008.

[12] SA. Song, HJ. Oh, BG. Kim, SS. Kim "Novel foaming methods to fabricate activated carbon reinforced microcellular phenolic foams". Composites science and technology, Vol. 76, pp 45-51, 2013.

[13] HG. Kim, DG.Lee "Dielectric cure monitoring for glass/polyester prepreg composites". Composite structures, Vol. 57, pp 91-99, 2002.

[14] JS. Kim, DG. Lee "Analysis of dielectric sensors for the cure monitoring of resin matrix composite materials". Sensors and actuators B, Vol. 30, pp 159-164, 1996.

[15] GD. Carvalho, E. Frollini, WND. Santos "Thermal conductivity of polymers by hot-wire method". Thermal conductivity of polymers. Vol. 62, pp 2281-2285, 1996.

[16] G. Woods "The ICI polyurethanes Book", New York: John Wiley & Sons, Vol. 35, 1987.